

CONF-810429--24

LA-UR -81-1440

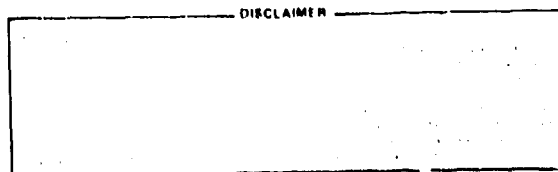
TITLE: PASSIVE RETROPULSE PROTECTION THROUGH ENHANCED OPTICAL BREAKDOWN

AUTHOR(S): Jerald V. Parker

MASTER

SUBMITTED TO: Conference on Optics, Santa Fe, NM, April 1981

University of California



By acceptance of this article, the publisher recognizes that the U.S. Government retains a nonexclusive, royalty free license to publish or reproduce the published form of this contribution, or to allow others to do so, for U.S. Government purposes.

The Los Alamos Scientific Laboratory requests that the publisher identify this article as work performed under the auspices of the U.S. Department of Energy.



LOS ALAMOS SCIENTIFIC LABORATORY

Post Office Box 1663 Los Alamos, New Mexico 87545

An Affirmative Action/Equal Opportunity Employer



Passive Retropulse Protection through Enhanced Optical Breakdown

Jerald V. Parker

University of California, Los Alamos National Laboratory
P. O. Box 1663, MS-455, Los Alamos, New Mexico 87545

Abstract

The potential for serious component damage due to reflected pulses increases rapidly with output energy. Optical materials for interstage isolators are not available for large 10.6 micron laser systems. We show that an excellent passive protection technique can be realized using optically induced gas breakdown in the high pressure laser medium. The reflected energy flux is reduced below the component damage threshold by using spatial overlap to increase the strength of the breakdown.

Introduction

As the output energy of short pulse CO₂ laser systems has increased in recent years, the potential for serious component damage due to reflected pulses has increased dramatically. Figure 1 illustrates schematically the source of the problem. Higher energy oscillator-amplifier systems are realized by adding larger diameter amplifier stages with appropriate beam expanding optics between stages. The net beam area expansion from oscillator to output increases roughly in proportion to the output energy. The laser-target interaction reflects a fraction of the incident energy ($\sim 5 - 10\%$) back through the system where the optical train now decreases the beam diameter and increases the energy flux. If nothing acts to limit the flux, the reflected energy incident on the oscillator will increase in proportion to the output energy.

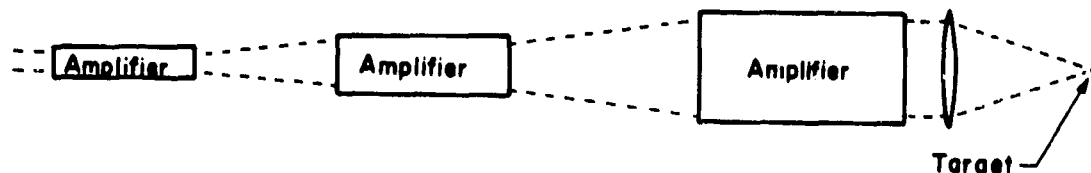


Figure 1 Schematic of high power laser system.

In visible and near infrared laser systems, this problem is commonly handled by interstage isolators which deflect the reflected pulse off the system axis. At this time the large aperture optical materials required to perform a similar function at 10.6 microns are not available.

We show that an excellent passive protection method can be developed using optically induced gas breakdown. The required large ratio of reverse to forward loss is achieved by utilizing the exponential dependence of loss rate on energy flux. The breakdown energy flux is reduced to a value below that which causes component damage by utilizing spatial overlap to increase the strength of the breakdown.

In the remainder of the paper, the dependence of optical breakdown on energy flux is derived for spatially uniform pulses with Gaussian time dependence propagating in an amplifying medium. This model is extended to treat the case of pulse propagation in the region near a mirror where spatial overlap of the pulse occurs. Finally, the predicted results are compared with experimental measurements performed on the final amplifier of the GEMINI laser system at the Los Alamos National Laboratory.

Optical Breakdown

When an electromagnetic wave is propagated through a gas containing free electrons, the electrons absorb energy through inverse bremsstrahlung. At sufficiently high intensities the electron temperature increases to the point that additional electrons are created leading to an exponential growth in electron density. The growth in electron density is accompanied by a proportionate loss of energy from the EM wave.

The calculation of optical breakdown is generally complicated, since electron generation rates must be corrected for recombination, diffusion and other losses. For the very high fields and short times considered here, the growth rate generally dominates any

loss process¹ and we may formulate a first order model of the avalanche process with the single equation

$$\frac{dn_e}{dt} = \frac{n_e}{\tau_g} \quad (1)$$

where n_e is the local electron density and τ_g is the growth time. The growth time is a function of the intensity of the electromagnetic field and is inversely proportional to the electron collision frequency (or equivalently, the neutral gas pressure for the weakly ionized gases considered here).

Thus the growth time can be written

$$\tau_g = \frac{P_0}{P} \tau_g^*(I) \quad (2)$$

where I is the intensity in W/cm^2 , P is the gas pressure and $\tau_g^*(I)$ is the growth time at pressure P_0 . The function $\tau_g^*(I)$ has been calculated theoretically by Rockwood² for a number of gas mixtures. His results for air and for a 3:1:1 He:CO₂:N₂ mixture are shown in Figure 2.

Given a temporal pulse shape and an initial electron density, equation 1 can be integrated numerically to obtain the final electron density after the pulse has passed a given point as a function of the total energy flux. Further, assuming a fixed energy loss per electron-ion pair the final electron density can easily be converted to energy lost from the pulse.

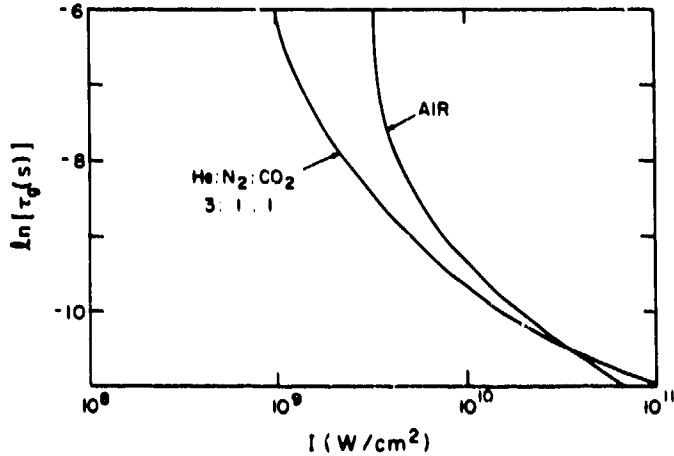


Figure 2. Growth time as a function of optical intensity (after Rockwood).

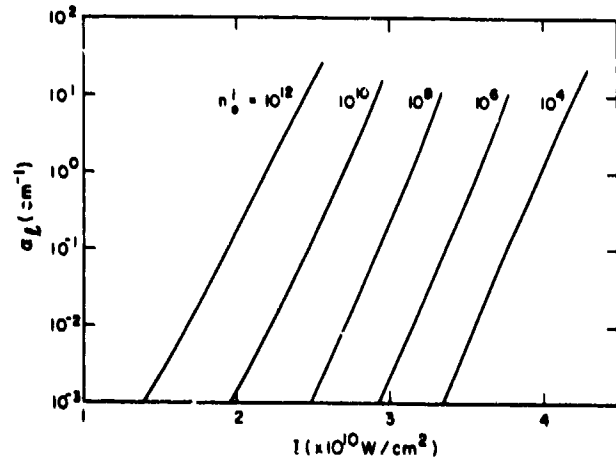


Figure 3. Calculate loss coefficient due to optical breakdown.

Figure 3 presents the results of such a calculation for a 3:1:1 (He:CO₂:N₂) laser mixture and for air at a pressure of 580 Torr. The incident pulse is assumed to have a Gaussian time dependence $I(t) = I_0 \exp[-(t/\tau)^2]$ with $\tau = 0.72$ ns (1.2 ns FWHM). The energy loss per ion-electron pair is assumed to be 30 eV. The fractional energy loss rate, α_l (cm^{-1}), is given as a function of the intensity I for various initial electron densities. For the loss rates of interest in high power laser system ($\alpha_l > 10^{-2} cm^{-1}$) the loss rate increases exponentially with energy flux.

Energy Flux Limits

The exponential dependence of loss rate on energy flux leads to a "limiting" or "equilibrium" energy flux for a given set of experimental conditions. If the energy flux tries to exceed this value the attenuation increases rapidly and restores the pulse back to the equilibrium energy flux condition.

Consider a converging beam as between stages in Figure 1. Ignoring loss processes for a moment a constant energy, converging beam produces an apparent gain in energy flux. That is, since

$$\frac{dE}{dx} = \frac{AdF}{dx} + \frac{FdA}{dx} = 0 \quad (3a)$$

then

$$\frac{1}{F} \frac{dF}{dx} = -\frac{1}{A} \frac{dA}{dx} = \alpha_c \quad (3b)$$

where A is the beam cross section area, F is the energy flux (J/cm²) and α_c is an effective gain experienced by the energy flux. In addition, the local gaseous medium may have a gain so that

$$\frac{dE}{dx} = \alpha_s E_s \quad (4)$$

where F is the energy flux (J/cm²) of the pulse, α_s the small signal gain (cm⁻¹) and E_s the saturation energy density (J/cm²).

Combining Equations 3 and 4 one obtains an effective gain

$$\alpha_{eff} = \frac{\alpha_s E_s}{F} - \frac{1}{A} \frac{dA}{dx} \quad (5)$$

The "limiting" energy flux, F_L , for a given situation is that value of F which makes the optical breakdown loss rate α_b equal to α_{eff} . The relation for F_L is an implicit one but a few iterations using Figure 3 and Equation 5 rapidly converges to a solution. Some typical values of the limiting flux are given in Table I. To confirm the original assertion that the "limiting" flux is a well-defined and practical quantity, consider case III of Table I. The "limiting" flux is 7.0 J/cm². If this flux were to suddenly increase to 8.0 J/cm² the loss rate would increase from 0.011 to 0.097 and the flux would tend back toward the "limiting" value in a characteristic distance $(\alpha_b - \alpha_{eff})^{-1} \approx 12$ cm. Thus, one expects that the local flux will not exceed the "limiting" value by more than 10 - 20 percent except possibly in regions where α_{eff} is increasing rapidly.

Table I Energy flux "limit" imposed by optical breakdown for some typical situations encountered in a short pulse CO₂ laser system. 3:1:1 (He:CO₂:N₂)

Gas	Pressure (Torr)	Initial Electron Density (cm ⁻³)	$\alpha_s E_s$ (J/cm ³)	$-\frac{1}{A} \frac{dA}{dx}$ (cm ⁻¹)	F_L (J/cm ²)
Air	760	10 ²	0	0.064	28.1
Laser	1800	10 ⁶	0	0.064	13.8
Laser	1800	10 ¹²	0.002	0.011	7.0
Laser	1800	10 ¹²	0.002	0	4.4

The results presented in Table I can be interpreted in terms of practical laser system design. Case 1 is typical of an interstage beam expander located in air. The "limiting" flux of 28 J/cm² greatly exceeds both the damage threshold for the best window materials (2 - 4 J/cm²) and the damage threshold for copper mirrors (5-10 J/cm²). Case 2 shows that moving the expander section inside the CO₂ amplifier (as in a multipass amplifier) still results in limiting energy fluxes exceeding the damage thresholds. Cases 3 and 4 are for propagation in a partially depleted laser medium with a residual gain of 1%/cm. Despite the high initial electron density, the limiting flux is still equal to or greater than the window damage threshold.

It is apparent, however, that the "limiting" flux in the high pressure amplifier is approaching a value at which damage could be eliminated.

Energy Flux Attenuation in an Overlap Region

Consider now the beam expander configuration shown in Figure 4. For a pulse of duration τ_p there will be a region in front of the convex mirror of length $c\tau_p/2$ where the local intensity will be doubled due to overlapping of the incident and reflected beams. Because the energy loss rate is so sensitive to intensity, an enhanced loss will occur in this region.

The spatial overlap geometry makes straightforward integration of the ionization rate equations difficult, particularly since drastic changes in pulse shape will occur as the pulse overlaps. We have, therefore, solved equations 1 - 3 numerically in the following manner.

The large signal gain limit is used since the "limiting" energy flux will greatly exceed the amplifier saturation flux in all cases of interest.

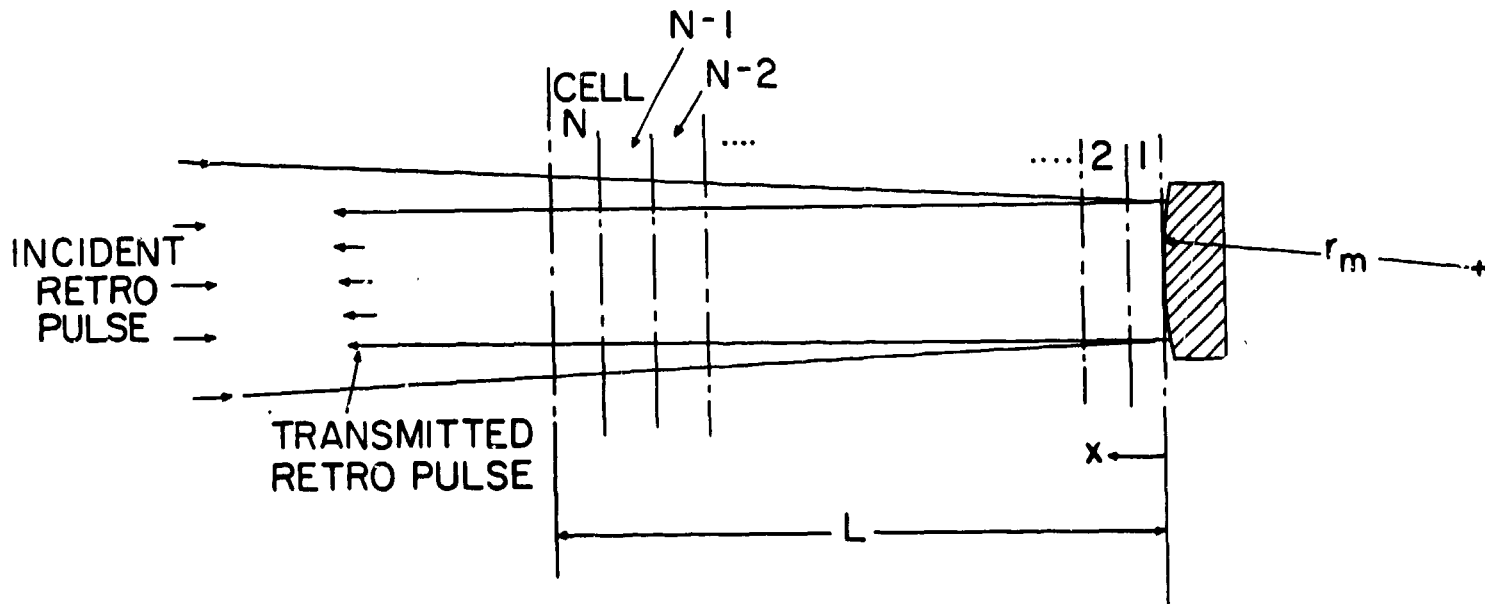


Figure 4. Geometry used to calculate optical breakdown with spatial overlap.

1. The beam is assumed to be of uniform intensity at each cross section.
2. A region of length L in front of the mirror is divided into N cells which are thin enough that there are only small changes in the physical variables from one cell to the next.
3. With each cell is associated an electron density $n_j^e(k)$, an intensity for the incident beam $I_f^j(k)$ and an intensity for the reflected beam $I_r^j(k)$, where k is the time step index ($t = \Delta t \cdot k$) and j is the cell index.
4. An input intensity of the form $I_f = A \exp(-t^2/t_p^2)$ is assumed for a pulse incident along the converging beam.
5. At each time step the following calculations are performed:
 - A) The change in electron density is calculated using Eqs. 1 and 2 where $I = I_f + I_r$.
 - B) The intensity of the forward and reflected beams are decreased in proportion to the change in electron density, assuming an energy loss of 30 eV per ion-electron pair created.
 - C) The incident beam intensity in each cell is transferred one cell closer to the mirror and the intensity increased to account for beam convergence.
 - D) The reflected beam intensity in each cell is transferred one cell farther from the mirror.
6. This procedure is repeated until the pulse has passed completely through the computational region.
7. The energies fluxes entering, leaving and reflecting from the mirror are calculated by integrating the intensity at these three locations over the duration of the pulse.

Calculations were carried out for only one pressure and mixture appropriate to the experimental situation discussed below. Extension of these results to other pressures can be made approximately by scaling the energy flux inversely with pressure. These results are not very sensitive to mixture ratio for the range of typical CO_2 laser mixes. Mixtures containing only rare gases or only diatomic gases will exhibit substantially lower or higher energy fluxes respectively and separate calculations would be required.

Referring to Figure 4, the calculations were carried out for the conditions $r_m = 63$ cm, $L = 56.25$ and $N = 750$. The cell size is then 0.75 mm and the time step 2.5 ps. The laser mix was 3:1:1 (He:CO₂:N₂) at a pressure of 1800 Torr.

Table 2 contains calculated mirror flux (F_M) and the flux leaving the breakdown region (F_R) for a number of parametric variations. For the first five cases the input pulse energy is chosen so that the converging beam would have a flux of 13.8 J/cm² at the mirror surface if no breakdown occurred (the "No breakdown" flux at the mirror is denoted F_0). Note that 13.8 J/cm² is the "limiting flux for this mixture and geometry and is thus a reasonable estimate of the flux which would exist at the mirror if no spatial overlap occurred.

Table 2. Calculated Energy Flux for Breakdown in an Overlap Region.
1800 Torr, 3:1:1 (He:CO₂:N₂)

Initial Electron Density	Pulse Width	F_0	F_M	F_M
cm ⁻³	HW/1/e	J/cm ²	J/cm ²	J/cm ²
10 ⁶	0.72	13.8	6.65	4.92
10 ⁹	"	"	5.31	3.21
10 ¹²	"	"	3.94	1.54
10 ⁶	0.48	13.8	6.04	3.64
10 ¹²	"	"	3.41	0.64
10 ⁶	0.72	27.6	6.51	2.52
10 ¹²	"	"	3.91	0.54

Cases 1 - 3 exhibit the influence of initial electron density. At the lower densities, typical of the background electron density in our electron beam sustained amplifier, the energy flux incident on the secondary mirror has been reduced to 6.65 J/cm², below the damage threshold for a high quality Cu mirror. The energy flux transmitted back toward the entrance window is still an unacceptably large 4.9 J/cm². Case 3 shows that one approach to reducing the transmitted energy flux further is to artificially increase the initial electron density in the breakdown region. At $n_{e1} = 10^{12}$ the transmitted flux is reduced below the damage threshold for NaCl windows.

The next two entries in Table 2 demonstrate that these results are not strongly dependent upon pulse duration although there is some reduction in the transmitted pulse energy for shorter pulse lengths because of the higher peak intensities. The last two entries demonstrate the interesting result that increasing the incident intensity decreases the transmitted energy flux.

The dependence of transmitted energy flux F_R on incident energy flux is shown in more detail in Figure 5. Both the energy flux seen by the mirror F_M and the flux leaving the computation region F_R are plotted vs the flux which would be incident on the mirror in the absence of optical breakdown, F_0 .

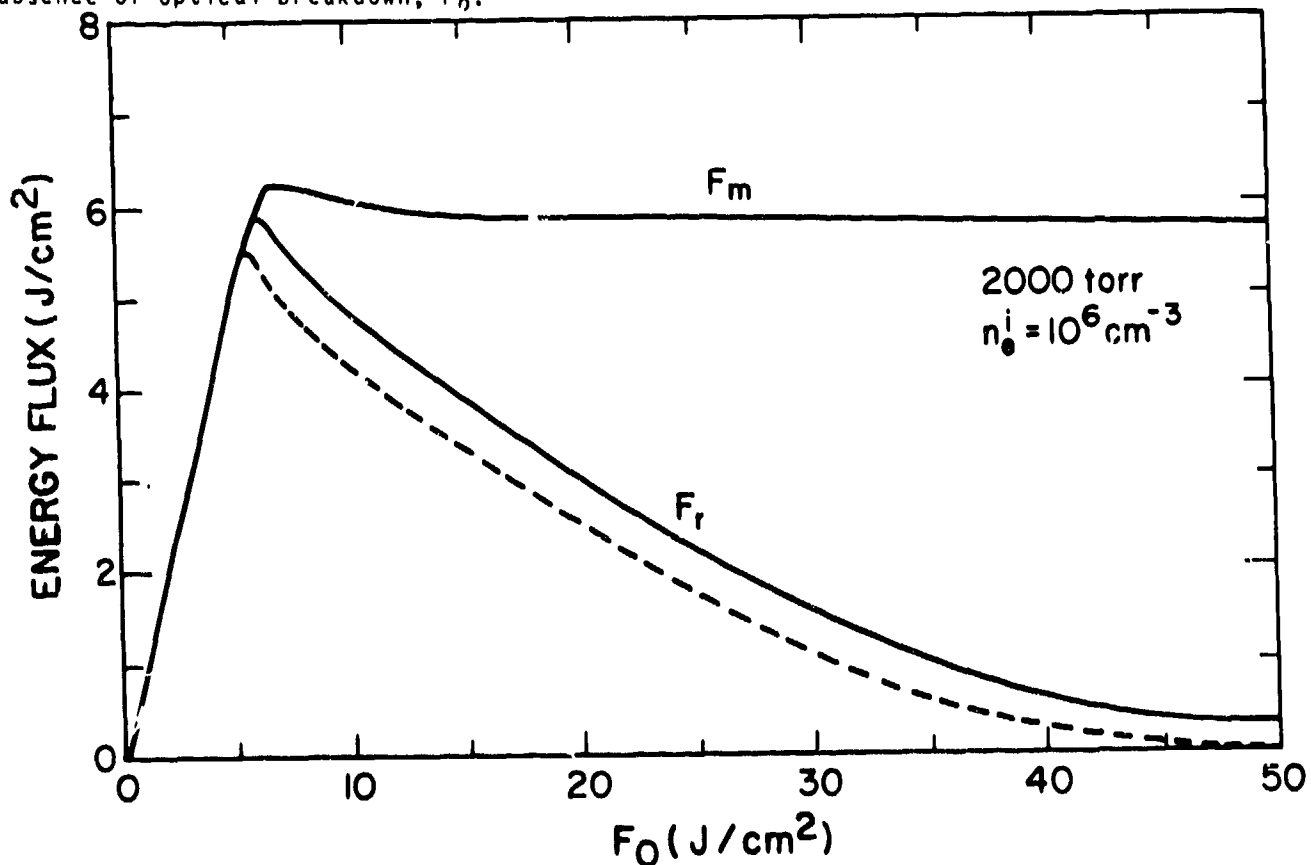


Figure 5. Calculate energy fluxes for optical breakdown with spatial overlap.

Both F_M and F_R are equal to F_0 until breakdown begins at $F_0 \approx 6 \text{ J/cm}^2$. As F_0 increases further the value of F_M reaches a nearly constant value of 6 J/cm^2 . The contrast, the reflected energy flux, F_R , begins to decrease rapidly after the breakdown threshold is passed and decreases to negligible levels for $F_0 \approx 50 \text{ J/cm}^2$.

This behavior can be understood by using the limiting flux concept discussed above. The gas mixture and optical geometry under consideration here correspond to the second case in Table 1. The pressure has been increased to 2000 Torr however so the limiting flux will be $.9 (13.8) = 12.4 \text{ J/cm}^2$. When the value of F_0 exceeds 12.4 J/cm^2 the incident pulse is beginning to ionize the gas in front of the mirror without benefit of the reflected pulse. At $F_0 = 50 \text{ J/cm}^2$ the limiting flux of 12.4 J/cm^2 is reached 32 cm in front of the mirror.

We conclude, (1) that overlap enhanced breakdown is a viable technique for retropulse protection; (2) it works best for strong retropulse, and (3) if the probability of weak retropulses cannot be sufficiently reduced in a system design then artificial enhancement of the electron density can provide satisfactory retropulse isolation.

Observations of Enhanced Optical Breakdown.

Retropulse attenuation in general agreement with the previous results has been observed on the GEMINI laser system at the Los Alamos National Laboratory. The final amplifier of GEMINI is a dual amplifier module utilizing a common cold cathode electron gun for the sustainer ionization. Each amplifier has an active volume $35 \text{ cm} \times 35 \text{ cm}$ in cross section and 200 cm long. To eliminate the need for high energy driver amplifiers the final amplifier is triple-passed. The beam overlap region occurs at the end of the first pass. The beam diameter at this mirror is 2 cm and the convex mirror has a focal length of 31.25 cm.

Retropulse energy measurements were performed during a series of target irradiation experiments. With a 300 J, 1.4 ns pulse incident on a flat, 2 mil thick polyethylene target the retropulse energy entering the final amplifier was $25 \pm 5 \text{ J}$ ($.025 \text{ J/cm}^2$). After passing through the amplifier the energy flux leaving the amplifier was less than 0.1 J/cm^2 .

The expected energy fluxes at several points inside the amplifier are given in Table 3. The first line shows the increase in flux which results from geometrical compression of the beam. In the second line the effects of a residual gain of $1.8\%/\text{cm}$ have been included. Since optical breakdown is not included here the calculated mirror flux is the quality F_0 referred to above.

On the third line the effects of optical breakdown have been included by reading the values of F_M and F_R from Figure 5 using the value $F_0 = 40 \text{ J/cm}^2$ from the second line. The observed energy fluxes are shown in the last line.

Optical breakdown in the region in front of the secondary mirror was verified by open shutter photographs. An intense ionization column is observed whose diameter is equal to the beam diameter (2 cm) and which extend $> 10 \text{ cm}$ out from the mirror surface. No visible emission is observed if no reflected pulse is formed (target blocked by diffuse absorber).

Comparison of the calculated and experimental results shows that a large part of the reduction in retropulse energy is accounted for by this simple model but that the measured energy flux is still substantially lower than the calculated value.

The most likely source of this discrepancy is the neglect of refractive effects. The measurement of reflected energy is made at a distance of 7 meters from the breakdown region so phase shifts across the breakdown plasma of $\approx 1 \lambda$ would be sufficient to reduce the measured energy.

Calculations of breakdown which include refractive effects correctly were prohibitively expensive so the following approximate calculation was carried out to see if refractive effects could explain the observations. The previously described calculations were modified to include both intensity and phase shift due to the local electron density. The integration of intensity to give reflected energy, F_R , was terminated when the phase shift due to free electrons reached 1λ .

The effect of refraction is to decrease F_R by $\sim 0.5 \text{ J/cm}^2$ for all values of F_0 above 6 J/cm^2 . The transmitted flux, including refraction, is shown by the dotted line in figure 5. Physically, this result is not unexpected. The most significant refractive effects occur during the final stages of the breakdown process when the electron density is high. Soon after refraction begins to have an effect, absorption comes into play and removes the rest of the pulse energy.

While the energy flux lost through refraction is small it becomes a dominant factor for large values of F_0 . For the conditions of the experiment reported above refraction reduces the reflected energy flux from 0.65 to 0.25. Considering the exploratory nature of this calculation it is likely that refraction effects contribute significantly to the discrepancy between the calculated and measured quantities presented in Table 3.

Acknowledgment

The research work leading to this paper was performed under the auspices of the US DOE.

References

1. Elliott, C. J., "Degradation of a Laser Medium Due to Ionization by a Laser Pulse," J. Applied Physics, Vol. 45, pp 345 - 349, 1974.
2. Rockwood, S. D., Canavan, G. H., and Proctor, W. A., "Intracavity Breakdown in CO and CO₂ Lasers," IEEE J. Quantum Elect., QE-9, p. 154 (1973); QE-9, p. 782 (1973).

Table 3. Comparison of calculated and experimental reflected energy flux at various locations in the Two Beam Laser System.
2000 Torr; Calc. 3:1:1 (He:CO₂N₂); exp. 3:1:1/4 He:CO₂:N₂)

Assumes Condition	Entering Amplifier	Collimating Mirror	F _{in}	F _M	F _R
No Gain No Breakdown	0.025	0.025	0.92	7.22	7.22
Gain No Breakdown	0.025	0.14	5/1	40.0	40.0
Gain Breakdown	0.025	0.14	5.1	6.4	0.65
Exp.	0.025	----	---	---	≤ 0.1